SI Appendix

Controlling orientational order in block copolymers using low intensity magnetic fields

Manesh Gopinadhan, Youngwoo Choo, Kohsuke Kawabata, Gilad Kaufman, Xunda Feng, Xiaojun Di, Yekaterina Rokhlenko, Lalit H. Mahajan, Dennis Ndaya, Rajeswari M. Kasi, Chinedum O. Osuji

Additional Materials and Methods

Materials. RM257 (1,4-Bis-[4-(3-acryloyloxypropyloxy)benzoyloxy]-2-methylbenzene), was a generous gift from Teledyne Scientific & Imaging, CA. 6OCB (4'-hexyloxy-4-cyanobiphenyl) mesogen was purchased from Sigma-Aldrich. The polylactide based material, NBPLA6k-b-NBLC20k, was synthesized by sequential ring-opening metathesis polymerization (ROMP) using a modified Grubbs catalyst.

X-ray scattering data collection and reduction. Data were recorded on a 2D gas-wire electronic detector at a distance of 80 cm from the sample plane, permitting access to scattering vectors q from 0.015 to 0.21 Å^{-1}. The system was calibrated using a silver behenate standard and the 2D scattering patterns were integrated azimuthally to obtain intensity, I versus scattering vector, $q = (4\pi/\lambda)\sin(\theta)$ where 2θ is the scattering angle. 2D data were processed using WSxM and Igor packages.[1]

Transmission Electron Microscopy. Samples were cryo-microtomed (Leica UC7) using a diamond knife. Approximately 100 nm thick sections were retrieved on 200 mesh TEM grids and stained in RuO$_4$ vapor for 7 mins before imaging (FEI Tecnai Osiris, 200 keV).

Differential Scanning Calorimetry. DSC was conducted using a Q200 instrument (TA Instruments) under N$_2$ flow at a heating/cooling rate of 2 °C/min.

Polarized Optical Microscopy. Samples were imaged under crossed polarizers using a Zeiss Axiovert 200M inverted microscope.

Atomic Force Microscopy. Atomic force microscopy measurements were performed with a Bruker Dimension Fastscan in tapping mode.

Rheology. Measurements were conducted on ARES-LS1 rheometer (TA Instruments) using 8 mm diameter parallel plates. Samples were initially heated above ODT to 90 °C. Dynamic temperature sweep experiments were performed on each sample at 2 % strain at an angular frequency of ω=1 rad/s.
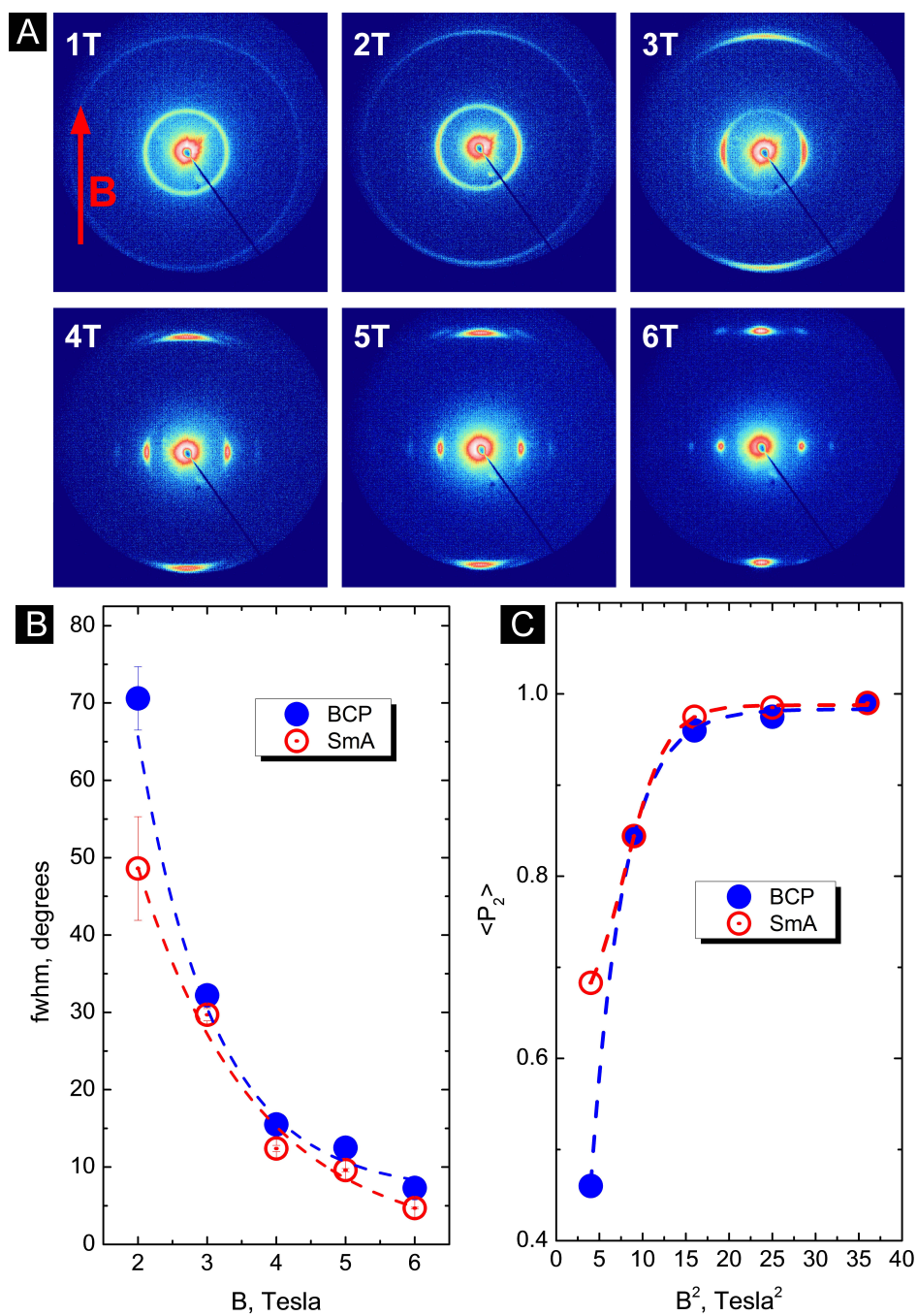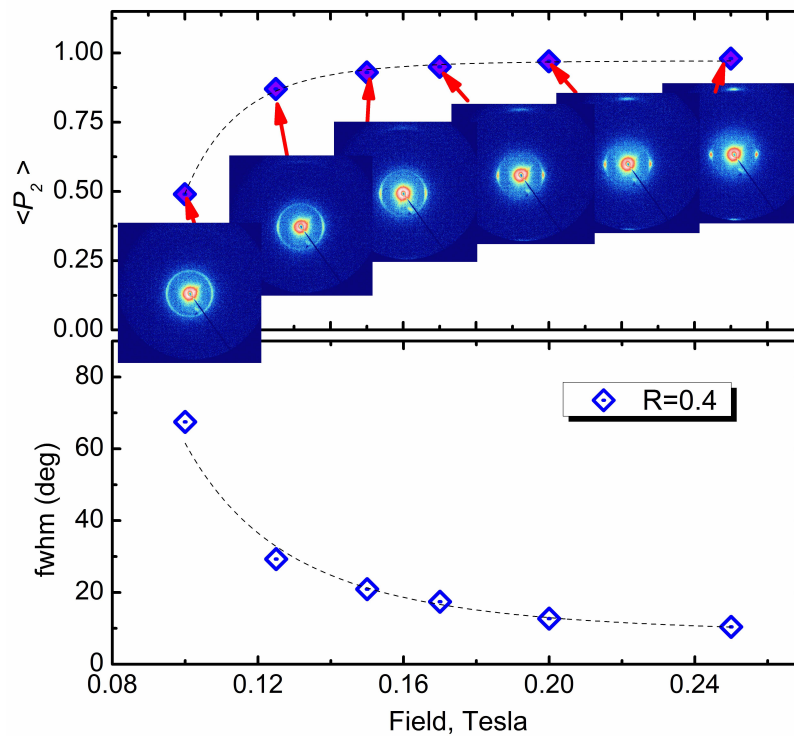
Fig. S1. A) 2D SAXS data of field dependence on alignment with full width at half maximum (fwhm) (B) and the corresponding $\langle P_2 \rangle$ of the neat diblock copolymer (2.4-11.2k) material estimated from Gaussian fits to the data (C). Dotted lines are logistic fits to the data.

http://www.pnas.org/lookup/suppl/doi:10.1073/pnas.1712631114/-/DCSupplemental
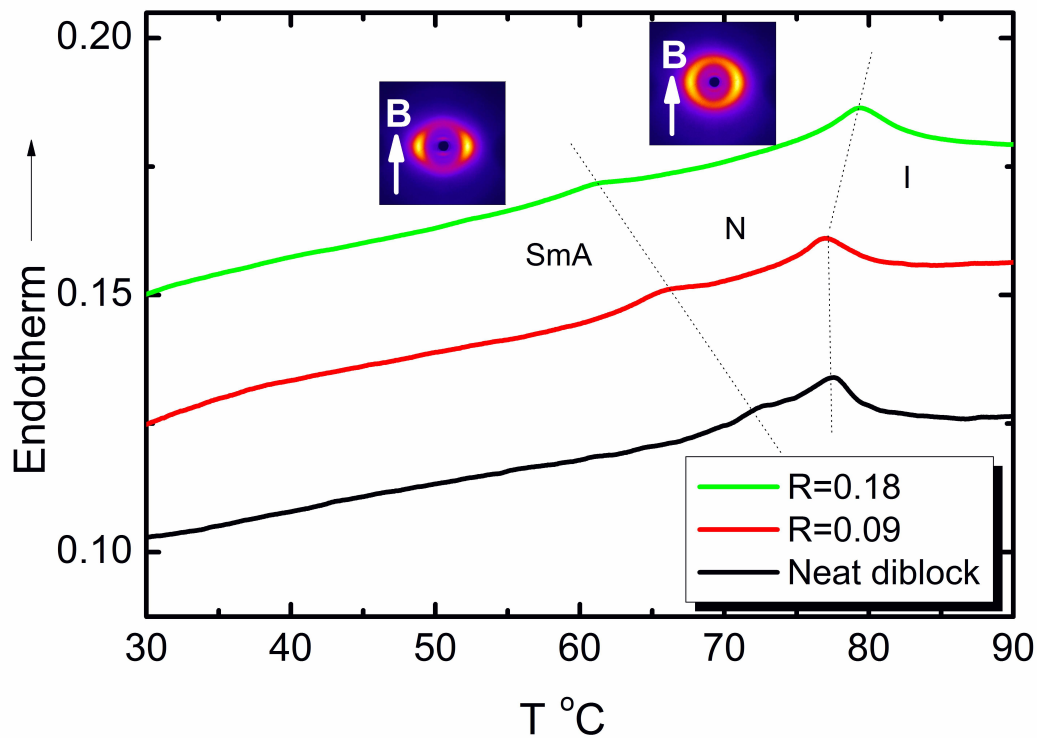
Fig. S2. DSC data of the pristine diblock PEO2.4-b-LC11.2K and the blend material with RM257 at stoichiometries, R=0.09 and R=0.18 are compared. It is clearly evident that the nematic window is broadening with the addition of free LC species. 2D WAXS data of the neat diblock material collected in the nematic and SmA phases during alignment at 1T is also shown.


Fig. S3. Field strength dependence of alignment for R=0.4 sample. 2D SAXS data are shown for field strengths indicated, along with the corresponding field dependence of the order parameter $\langle P_2^{BCP} \rangle$ (Top) and fwhm (Bottom). The sample shows alignment saturation around 0.2 T at a cooling rate of 0.1 $^\circ$C/min. This can be compared with the 0.5 T saturation for R=0.18 aligned at the same cooling rate.
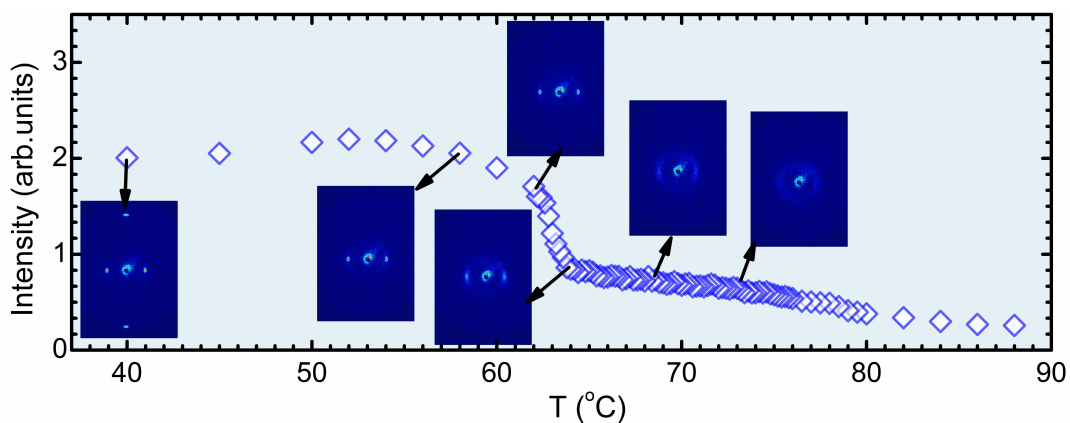
Fig. S4. Intensity (and selected 2D SAXS patterns) of the BCP superstructure of the blend material at a stoichiometric ratio of R=0.18 recorded during alignment at 1T. During cooling, the material shows weak alignment in the nematic state $\sim$ 64-73 $^{\circ}$C and an enhancement upon entering SmA state.
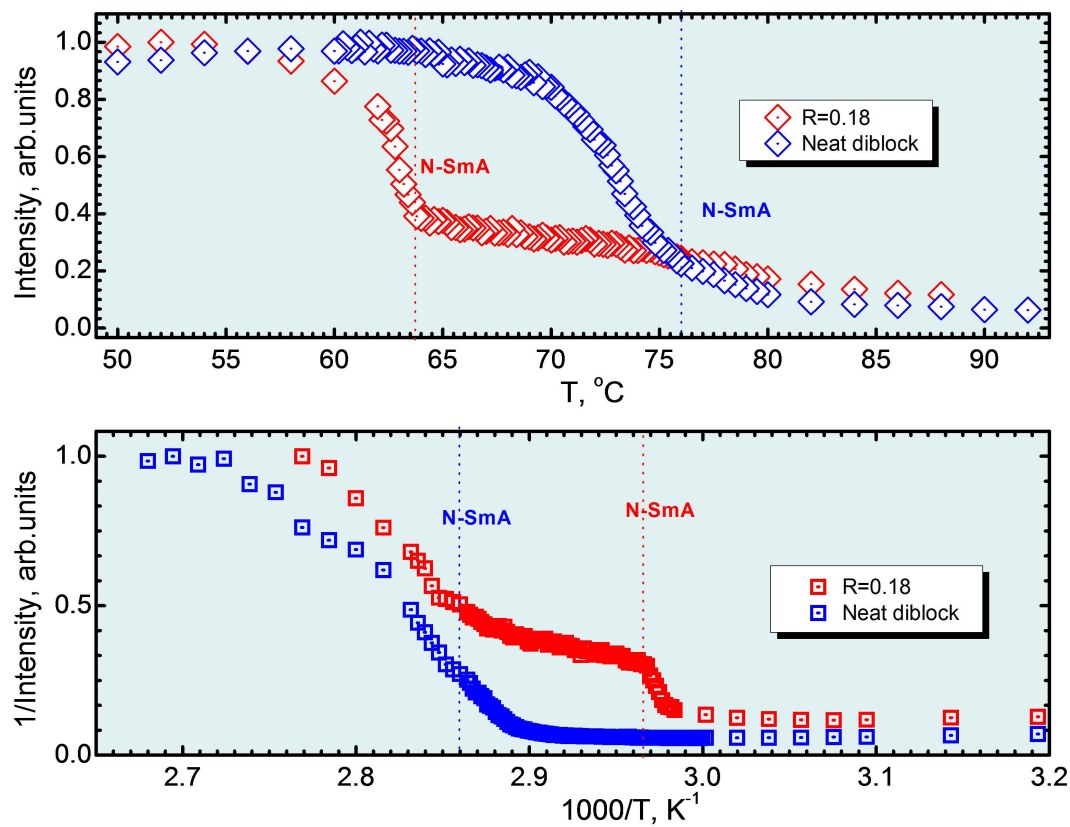

Fig. S5. Peak intensity comparison between neat BCP (EO-MA/LC) superstructure and the BCP blended with RM257 at a stoichiometric ratio of R=0.18 (top) and the bottom shows corresponding inverse intensity plots. A broader nematic window and a significant shift ($\sim$12 $^{\circ}$C) of the N-SmA transition temperature were observed for the blend.
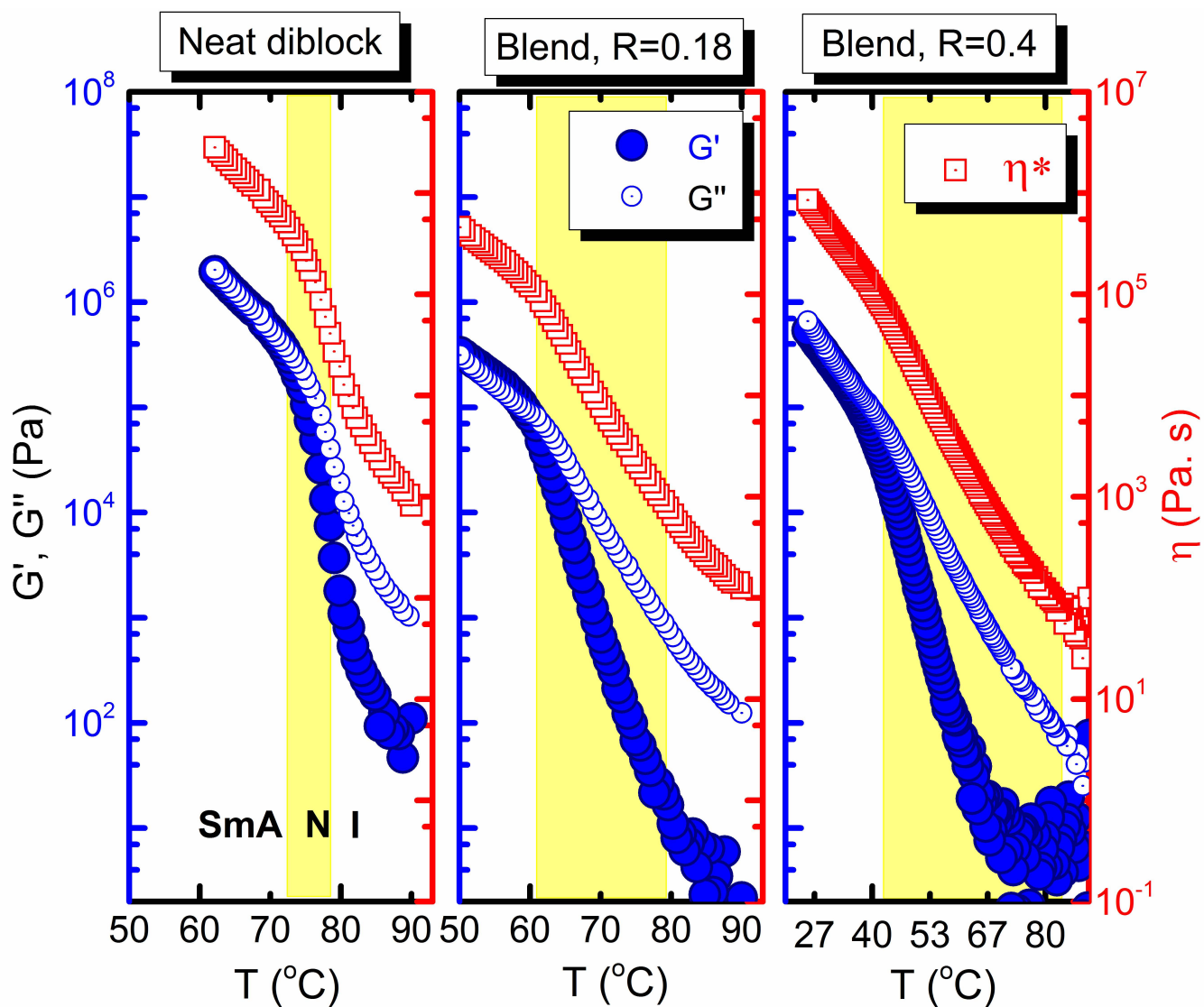
Fig. S6. a) Comparison of the rheology data of the neat diblock, and the blend materials at stoichiometries R=0.18 and R=0.4. Overall viscosity in the nematic window decreases with increase in stoichiometry. For R=0.4, G′, G″ and η show more gradual increase with temperature and the crossover temperature is much lower compared to R=0.18 sample.
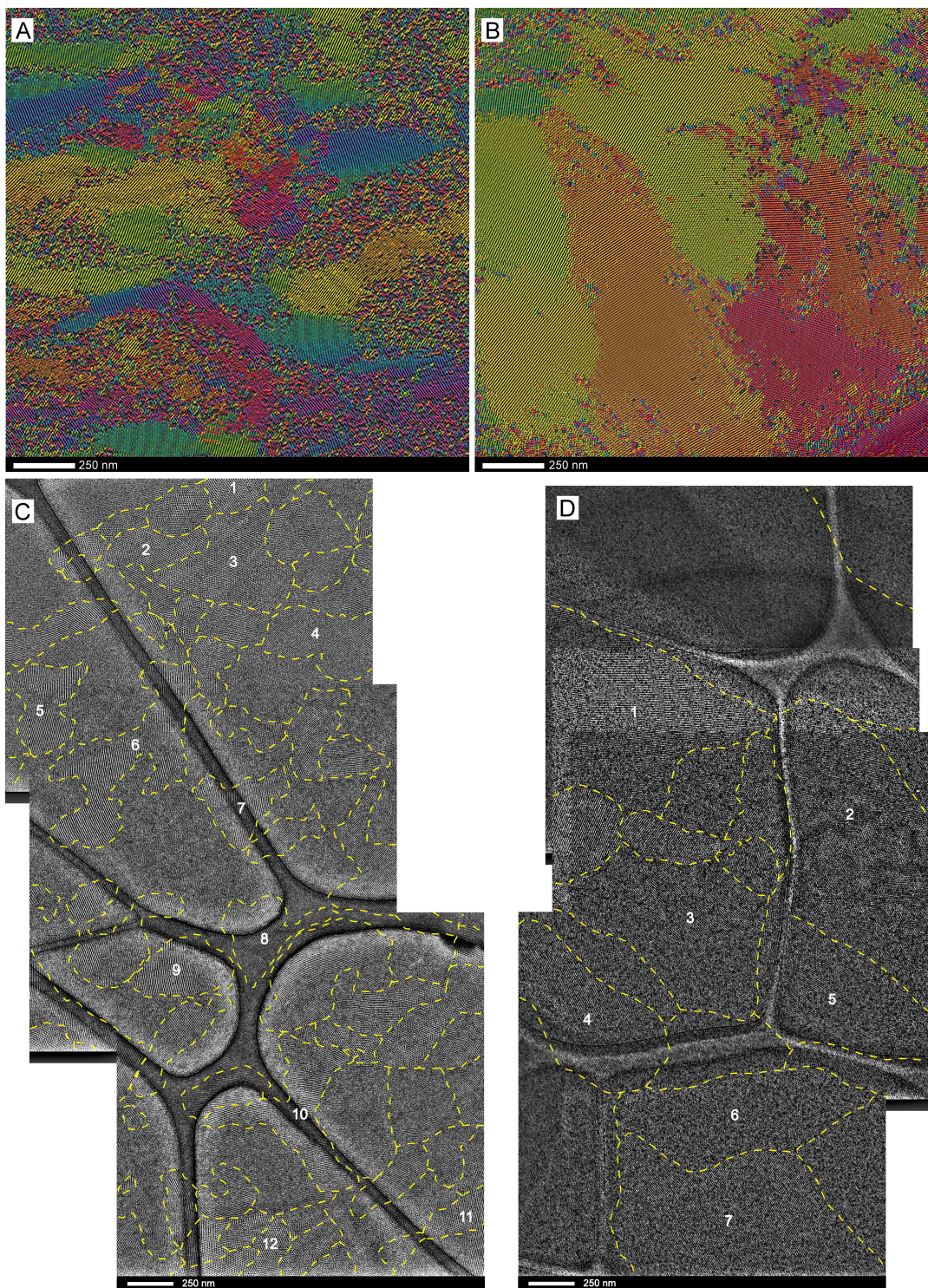
Fig. S7. A, B) Representative TEM images showing larger area views of non-aligned neat system and R=0.18 blend samples. PEO domains appear dark due to RuO_4 staining. The average grain size of the blended samples is larger than in the neat samples. The images span 4 μm^2 areas and are overlaid with a false color mapping as a visual guide. C, D) TEM images of neat and R=0.18 blend samples, respectively, obtained by stitching together separate images to provide a yet larger area view. Grain boundaries have been manually identified where the contrast and morphology permit such, as indicated by the dashed yellow lines. A subset of grains are identified by numerical labels. The small feature size and poor electron density contrast (in part due to added mesogen - cf. R=0.075 data in Fig. S9) make it difficult to identify all grain boundaries, and particularly for smaller grains. Nevertheless, the difference in grain size between the neat and blend sample can be clearly seen.
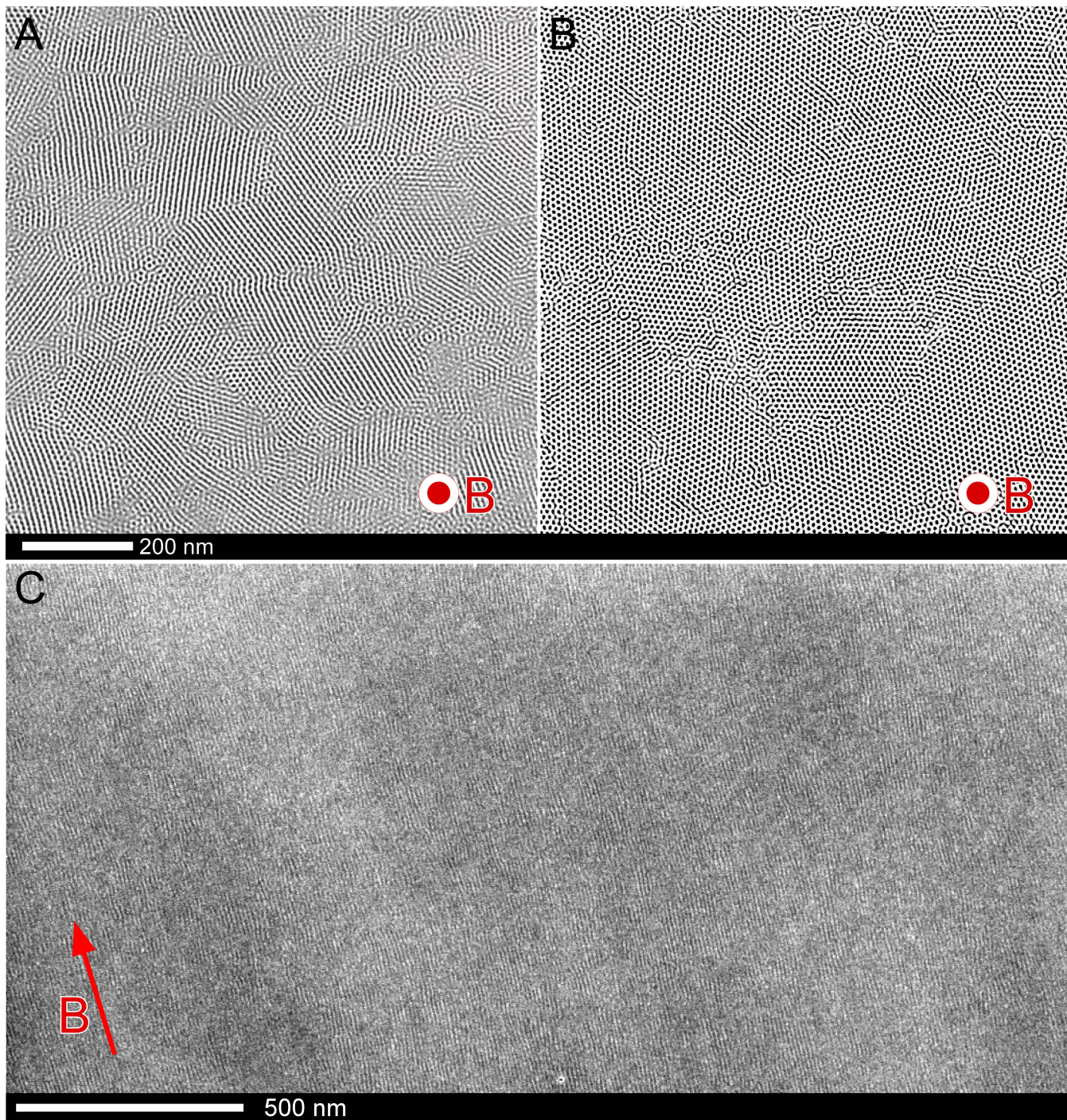
Fig. S8. A) and B) TEM of neat diblock aligned at 6 T and the R=0.18 blend aligned at 1 T, respectively, when viewed along the field direction. Both samples were aligned at a cooling rate of 0.1 °C/min. C) TEM viewed perpendicular to the field shows alignment of R=0.18 blend produced at 1 T at a cooling rate of 0.1 °C/min. The image shows continuity of microdomains over roughly 1.5 μm distances.
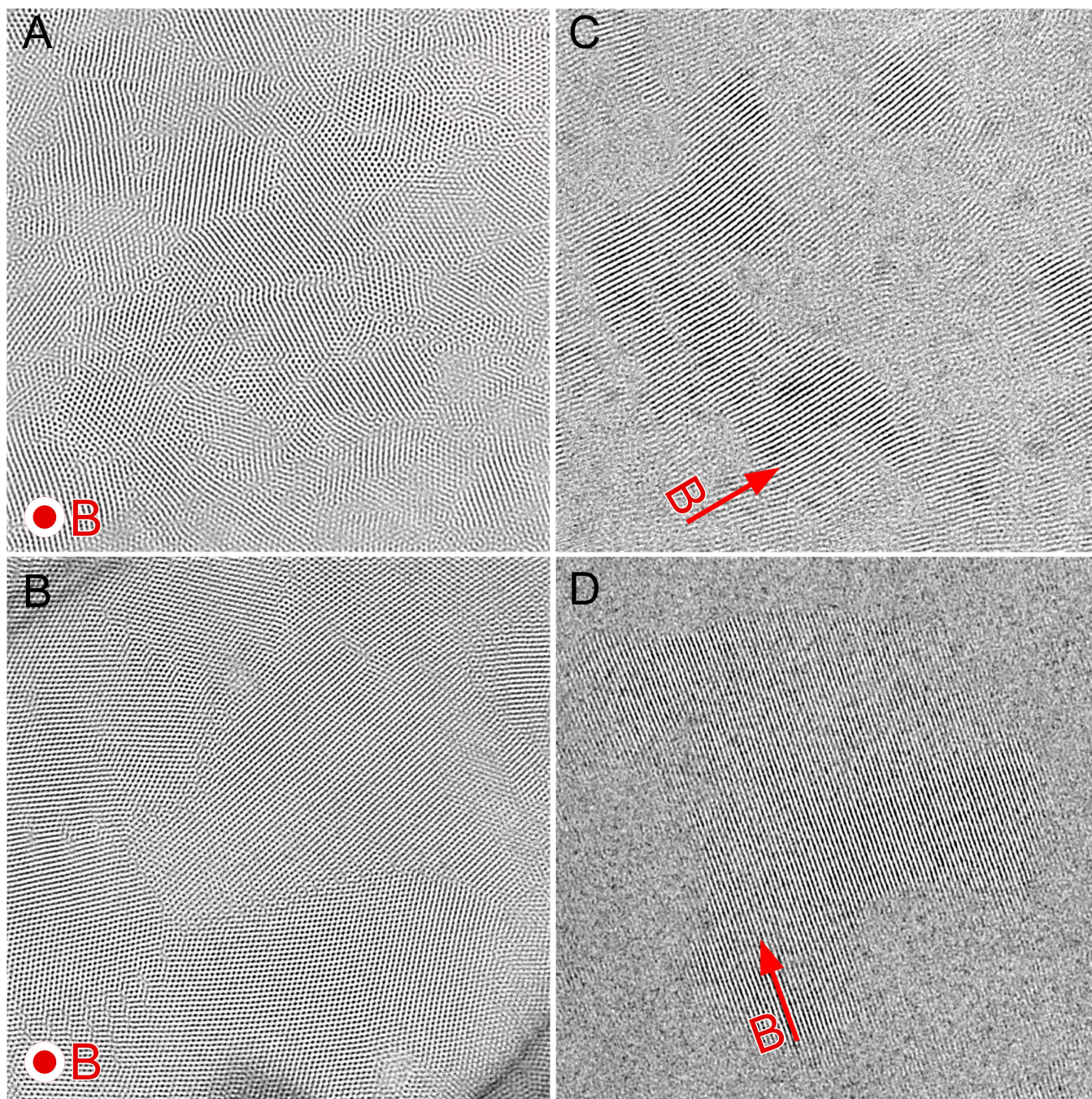
Fig. S9. TEM of neat diblock (A, C) compared with R=0.075 sample and (B, D) viewed parallel and perpendicular to the applied field respectively for each case. The grain sizes observed in the blend are larger than those observed in the neat material. The neat sample was aligned at 6 T while the blend sample was aligned at 1 T. Both samples were subjected to a cooling rate of 0.1 $^\circ$C/min. The images span 1 μm^2 area. There is better electron density contrast for R=0.075 relative to the R=0.18 blend.
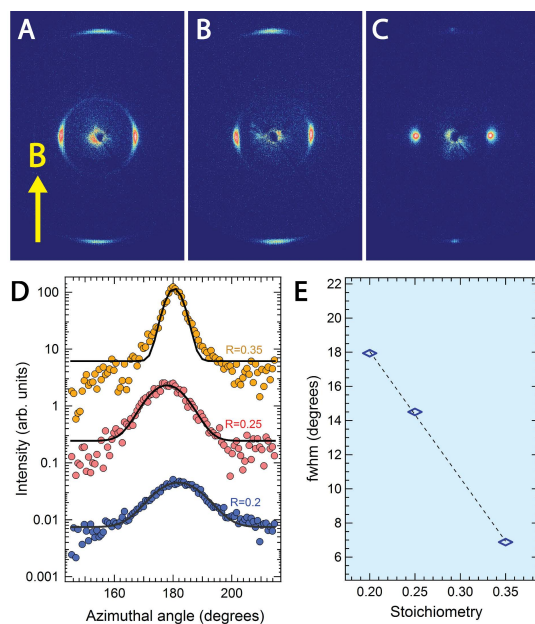
Fig. S10. Field alignment of PEO-b-LC material after blending with 6OCB at different stoichiometries. (A-C) R=0.2, 0.25 and 0.35 aligned at a cooling rate of 0.1 °C/min at 0.75T. D) and E) Corresponding azimuthal intensity profiles of the BCP superstructure fitted with Gaussian function (black solid lines) and the obtained fwhm values.
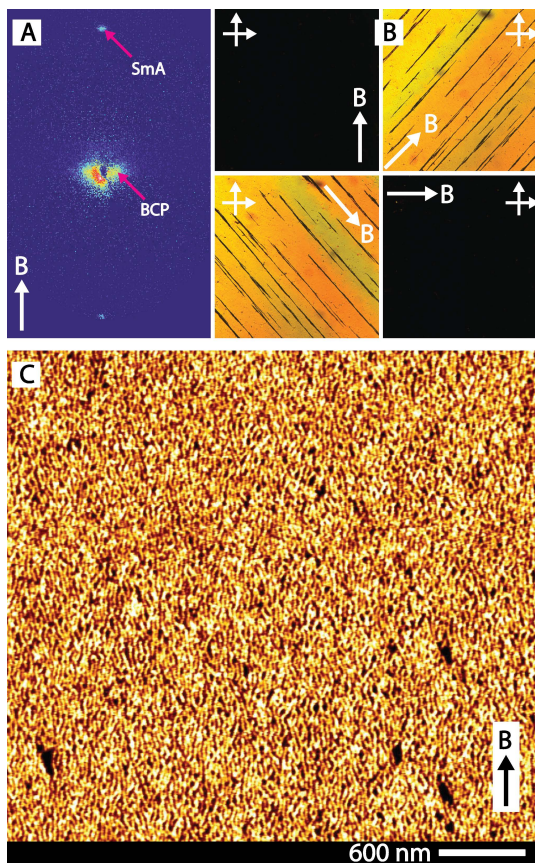
Fig. S11. Field alignment of PEO5-b-LC25 high MW material after blending with 6OCB at a stoichiometry of 0.35. A) SAXS data collected after cooling in 1 T field at a cooling rate of 0.1 °C/min. B) POM data on the polymer film (10 microns thick) blended with Co-particles display strong optical anisotropy. The sample was subjected to 1 T field. The particle chains are assembled in the field direction. AFM image indicates that cylindrical domains are aligned in the direction of the field (C).
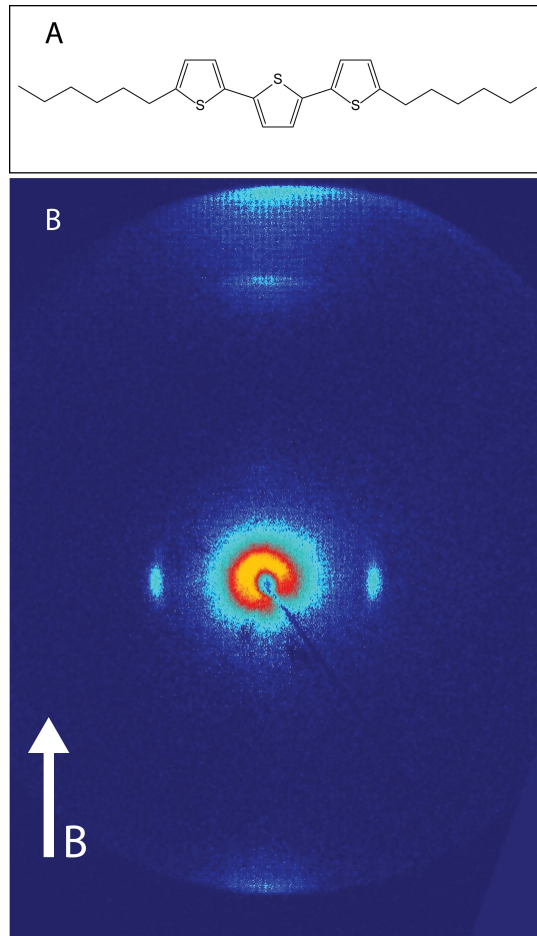
Fig. S12. PEO-MA/LC with a ter-thiophene mesogen (5,5"-dihexyl-2,2':5',2"-terthienyl) at a stoichiometry of R=0.2 aligned at 1T with 0.1 °C/min. A) chemical structure of the mesogen B)SAXS data of the blend material.
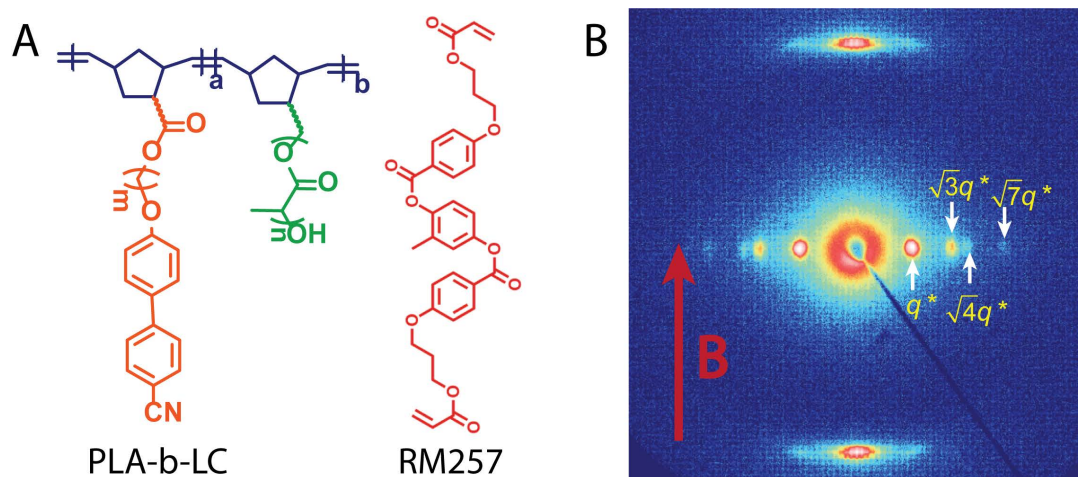
Fig. S13. Field alignment of a cylinder forming LCBCP (NBPLA6k-b-NBLC20K). A) In this polymer architecture, PLA side chains and cyanobiphenyl mesogens are attached to the norbonene backbone (NB). RM257 mesogens are complexed with the block copolymer at a stoichiometry of 1.2. B) SAXS data of the aligned sample subjected to a field of 0.75 T. Cooling rate was chosen to be 1 °C/min.

1. Ilavsky J, Jemian PR (2009) Irena: tool suite for modeling and analysis of small-angle scattering. J. Appl. Crystallogr. 42(2):347–353.